Propagation characteristics of laser light under the influence of atmospheric disturbance

Genta Masada

Quantum ICT Research Institute, Tamagawa University
6-1-1 Tamagawa-gakuen, Machida, Tokyo 194-8610, Japan

Propagation characteristics of laser light under the influence of atmospheric disturbance

Genta Masada

Quantum ICT Research Institute, Tamagawa University

6-1-1 Tamagawa-gakuen, Machida, Tokyo 194-8610, Japan

E-mail: g.masada@lab.tamagawa.ac.jp

Abstract—**Quantum illumination is a theory for detecting the existence of targets with high sensitivity by using quantum entanglement of light. In the quantum illumination, one of the light waves in the entangled state is emitted toward the target in the atmospheric disturbance. Therefore, it is extremely important to investigate the propagation characteristics of light waves under the influence of atmospheric disturbances towards the study of quantum illumination. In this study, as an example of atmospheric disturbance, we investigated the propagation characteristics of laser light in an atmosphere with thermal fluctuation and air flow. It was clarified experimentally that thermal fluctuation has a significant effect on the intensity distribution of light waves, but the effect of air flow is small.**

I. INTRODUCTION

Quantum illumination is a theory for detecting the existence of targets with high sensitivity by using two light waves with the properties of quantum entanglement [1], [2], [3]. One of the entangled light waves is emitted toward the target and its reflection is received by the receiver. The other light wave is input directly to the receiver. In the receiver, it is possible to determine the presence or absence of a target with high sensitivity by performing quantum optimum measurement on both light waves. It is also expected that the error probability when detecting a target will be improved even under the influence of atmospheric disturbances such as optical loss and noise. Initially, the Bell state, which is an entangled photon pair, was proposed as a quantum entanglement light source [1]. Subsequently, Tan, *et al*. considered quantum illumination using a Gaussian state such as a two-mode squeezed vacuum state, which has the property of macroscopic quantum entanglement [2]. They showed that under certain conditions, the two-mode Gaussian state had better target detection performance than the single-mode laser.

We are studying quantum illumination using two-mode squeezed light [4]. When applying quantum illumination to radar systems, quantum entanglement light is used in outdoor environments with the effects of atmospheric disturbances. Therefore, it is necessary to obtain detailed knowledge about the effects of atmospheric disturbances on the propagation characteristics and quantumness of light waves. In previous studies, we focused on the effects of fog that obstruct visibility as an example of atmospheric disturbances [5], [6]. Experiments with single-mode squeezed light have shown that the effect of uniform fog on light waves is significant energy attenuation caused by Mie-scattering.

In this study, we focused on the effects of thermal fluctuation and air flow as atmospheric disturbances. Random temperature changes and air flow in the atmosphere are thought to be factors that cause fluctuations in the refractive index. There have been many research reports on the propagation characteristics of light waves in atmospheric disturbances [7], [8], [9]. It is known that atmospheric disturbance causes beam wonder in which the optical axis changes randomly, fluctuation of intensity distribution, and deterioration of beam quality. The purpose of this study is to investigate the effects of thermal fluctuations and air flow on the propagation characteristics of light waves. In an atmosphere with thermal fluctuation and airflow, the laser beam was propagated, and the intensity distribution and optical coherence were investigated.

II. EXPERIMENTAL METHOD

Fig. 1 (a) shows an experimental setup for investigating the effects of atmospheric disturbances on the propagation characteristics of laser light. In this study, we investigated the effects of thermal fluctuation and airflow as atmospheric disturbances. A continuous wave He-Ne laser with a wavelength of 633 nm was used as a light source. The height of the optical axis of the laser beam was set to 4 inches from the surface of the optical table. The laser light was reflected by the mirrors (Ms) and split into signal light and reference light by the beam splitter BS_1. First, only signal light was used to measure the fluctuation of the intensity distribution when affected by atmospheric disturbances. At this time, the reference light was blocked by the block. First, the hot plate shown in Fig. 1 (b) was installed in the optical path of signal light to generate thermal fluctuation. The height from the heated surface of the hot plate to the optical axis was 52 mm. The beam profiler (Ophir, BM-USB-SP928-OSI) was installed at a position 900 mm away from the center of the hot plate, and the intensity distribution of the signal light was measured.

Next, a blower (Dyson, Supersonic Ionic) shown in Fig. 1 (c) was installed in the optical path of the signal light to generate an air flow. This device is originally used as a hair dryer and can generate a warm air flow. However,

28
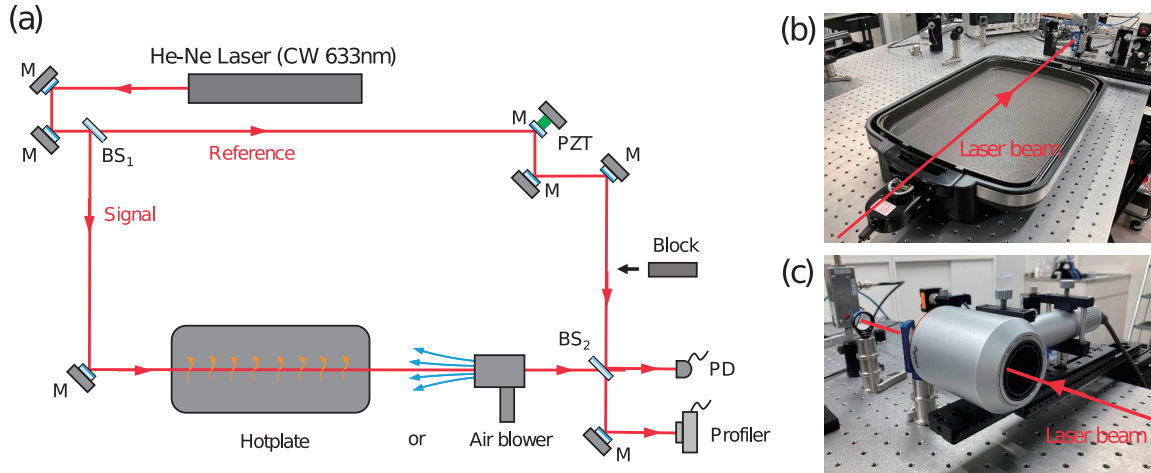
Fig. 1. Optical experiment setup to investigate the propagation characteristics of a laser beam under the influence of atmospheric disturbance . (a) Overview of the experimental equipment, (b) Photograph of the hot plate used to generate temperature fluctuations, and (c) Air blower used to generate air flow on the optical axis.
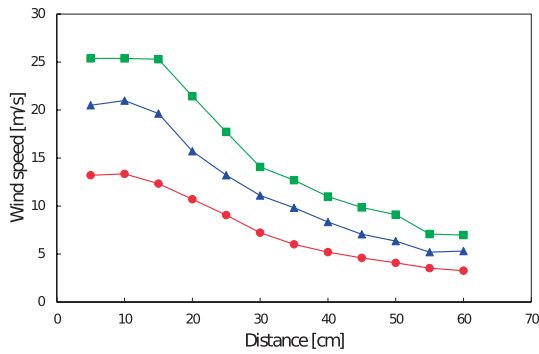
Fig. 2. The measurement result of the wind speed of the air flow generated by the air blower. Red circles, blue triangles, and green squares indicate measurement results at the air volume levels 1, 2, and 3, respectively.

in this experiment, it was used to generate an air flow with the same temperature as the external atmosphere. There is a hole in the wind blowing part of this blower, and signal light can pass through the center of the blower. Therefore, it is possible to measure the intensity distribution when the signal light is affected by the head wind symmetrical to the optical axis. Fig. 2 is the result of measuring how the wind speed changes depending on the distance from the end face of the blower. The blower used in this experiment can change the air volume level in three stages. It can be seen that the wind speed increases as the air volume level increases. In addition, it can be seen that the wind speed is the fastest within a range of about 10 cm from the end face of the blower, and the wind speed decreases as the distance from the end face increases. When the air volume is level 3, the wind speed near the end face of the blower reaches 25 m/s, which is equivalent to 90 km/h.

Next, the signal light affected by the atmospheric

disturbance and the reference light that passed through the free space were combined by the beam splitter BS_2, and the intensity of the interference light was observed by the photodetector PD. A mirror attached to the piezo transducer (PZT) was installed in the optical path of the reference light. By applying a triangular wave voltage to the PZT, the relative phase difference between the signal light and the reference light was changed. By this operation, it is possible to observe the interference signal. In this experiment, we also investigated the effects of thermal fluctuation and airflow on light interference.

III. PRELIMINARY EXPERIMENT FOR MEASURING THE INTENSITY DISTRIBUTION OF THE LASER BEAM

Fig. 3 shows the intensity distribution of signal light for 4 frames at the start of measurement. Intensity distributions (a) when there is no influence of atmospheric disturbance, (b) when the temperature on the optical axis is set to 50 °C, and the influence of thermal fluctuation is given, and (c) when the airflow of air volume level 3 are given. The size of the active area of the image sensor of the beam profiler is 5.3 mm x 7.1 mm. The beam profiler is connected to a PC and is controlled by software (Ophir, BeamMic). The exposure time of the beam profiler was set to 0.078 ms and the gain was set to 3 dB. By the function of the software, it is possible not only to acquire the data of the intensity distribution but also to obtain the numerical value of the centroid and the beam size by automatic calculation. When the intensity distribution of the beam in the two-dimensional plane is expressed by $I(x,y)$, the centroids X and Y in the horizontal and vertical directions are calculated by

$$X = \frac{\iint_D I(x,y)\,x\,dx\,dy}{\iint_D I(x,y)\,dx\,dy} \qquad (1)$$
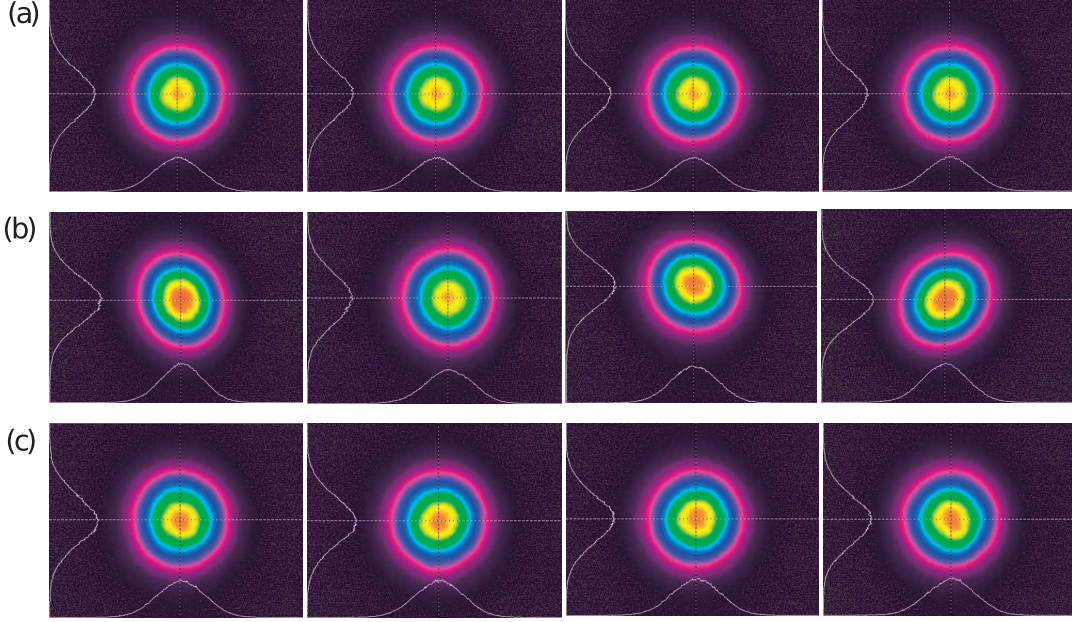
Fig. 3. Beam profile measurement results. As an example, four frames at the start of measurement are shown. These are the measurement results under (a) no influence of thermal fluctuation and air flow (b) the influence of thermal fluctuation (c) the influence of air flow, respectively.

and

$$Y = \frac{\iint_D I(x,y)\, y\, dx\, dy}{\iint_D I(x,y)\, dx\, dy}, \qquad (2)$$

respectively. The horizontal and vertical beam sizes D4σ_x, D4σ_y are also calculated by the following definition formulas

$$D4\sigma_x = 4\sqrt{\frac{\iint_D I(x,y)\, (x-X)^2\, dx\, dy}{\iint_D I(x,y)\, dx\, dy}} \qquad (3)$$

and

$$D4\sigma_y = 4\sqrt{\frac{\iint_D I(x,y)\, (y-Y)^2\, dx\, dy}{\iint_D I(x,y)\, dx\, dy}}, \qquad (4)$$

respectively. These correspond to four times the standard deviation σ_x and σ_y. The integration area D in the above equations experimentally corresponds to the active area of the image sensor of the beam profiler. The centroid and beam size were analyzed at the same time when observing the intensity distribution. Therefore, the frame rate was limited to about 15 Hz.

When there is no influence of atmospheric disturbance, there is almost no change in the centroid position or shape of the intensity distribution as shown in (a). The intensity profiles shown on the vertical and horizontal axes are approximated by a Gaussian distribution. It can be seen that under the influence of thermal fluctuation, the centroid position of the beam indicated by the intersection of the dotted lines in the vertical and horizontal directions, and the beam shape and size fluctuate as shown in (b). It can also be seen that the centroid position hardly changes when affected by the air flow, but the beam shape and

size fluctuate slightly as shown in (c). In this study, such measurements were repeated while changing the conditions of atmospheric disturbance.

IV. EXPERIMENTAL RESULTS UNDER THE INFLUENCE OF THERMAL FLUCTUATION

When the laser beam passed through the atmosphere with thermal fluctuation, random movement of the intensity distribution and distortion as shown in Fig. 3(b) were observed. The measurement results of the intensity distribution are shown in various expressions. Fig. 4 shows the centroid position of the intensity distribution in a scatter plot. The horizontal axis (vertical axis) is the centroid X (Y) calculated from the intensity distribution. Similarly, Fig. 5 is a scatter plot of the beam size of the laser beam. The horizontal axis (vertical axis) is the beam size D4σ_x (D4σ_y) calculated from the intensity distribution. The measurements were made 1000 times. In both figures, (a) is the result of measurement at room temperature of 24 °C without operating the hot plate. (b), (c) and (d) represent the measurement results when the atmospheric temperature on the optical axis is heated to 30 °C, 40 °C and 50 °C by the hot plate.

Fig. 6 shows the frequency distribution of the centroid position of the laser beam affected by thermal fluctuation, which was calculated using the measurement results of Fig. 4. Similarly, Fig. 7 is the frequency distribution of beam size calculated using the measurement results of Fig. 5. In both figures, the temperatures on the optical axis of the beam are (a, e) room temperature 24 °C, (b, f) 30 °C, (c, g) 40 °C, and (d, h) 50 °C, respectively. In
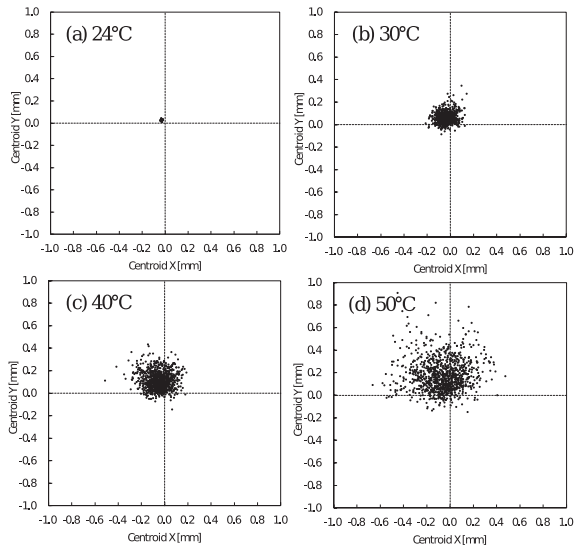
Fig. 4.   Measurement result of centroid position in the intensity distribution of the laser beam affected by thermal fluctuation. The temperatures on the optical axis of the beam are (a) room temperature 24 °C, (b) 30 °C, (c) 40°C, and (d) 50 °C, respectively.
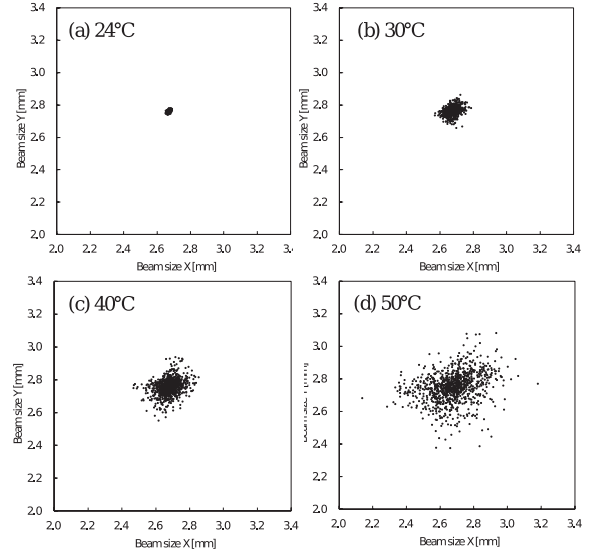
Fig. 5.   Measurement result of beam size in the intensity distribution of the laser beam affected by thermal fluctuation. The temperatures on the optical axis of the beam was (a) room temperature 24 °C, (b) 30 °C, (c) 40°C, and (d) 50 °C, respectively.
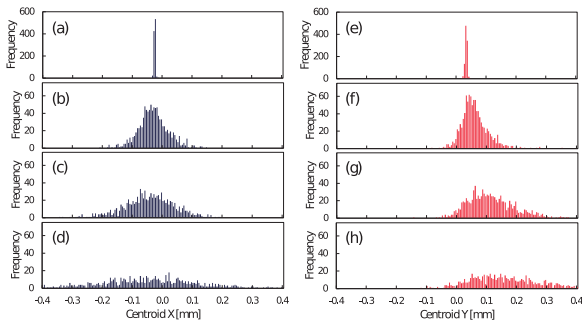
Fig. 6.   Frequency distribution of centroid in the intensity distribution of the laser beam affected by thermal fluctuation. The temperatures on the beam optical axis are (a, e) room temperature 24 °C, (b, f) 30 °C, (c, g) 40 °C, and (d, h) 50 °C, respectively. (a) to (d) show the result of centroid X, and (e) to (h) show the result of centroid Y.
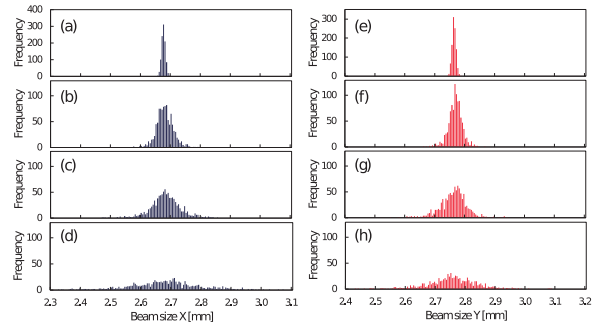
Fig. 7.   Frequency distribution of beam size in the intensity distribution of the laser beam affected by thermal fluctuation. The temperatures on the beam optical axis are (a, e) room temperature 24 °C, (b, f) 30 °C, (c, g) 40 °C, and (d, h) 50 °C, respectively. (a) to (d) show the result of centroid X, and (e) to (h) show the result of centroid Y.
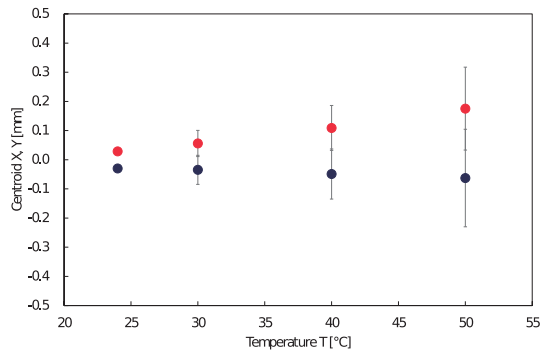
Fig. 8.   Measured values of the centroid position in the intensity distribution of the laser beam affected by thermal fluctuation. The blue circles (red circles) are the average value of centroid X (Y), and the error bars represent the standard deviation.
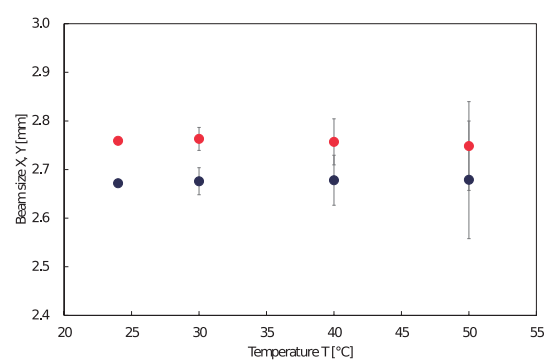
Fig. 9.   Measured values of the beam size of the laser beam affected by thermal fluctuation. The blue circles (red circles) are the average values of centroid X (Y), and the error bars represent the standard deviation.

Fig. 6, (a) to (d) ((e) to (h)) represent the frequency of centroid X (Y). Similarly, in Fig. 7, (a) to (d) ((e) to (h)) represent the frequency of beam size X (Y).

Fig. 8 and Fig. 9 are a summary of the measurement results of centroid and beam size under the influence of themal fluctuation. In Fig. 8, the blue circle (red circle) is the average value of centroid X (Y), and the error bar indicates the magnitude of the standard deviation. Similarly, in Fig. 9 , the blue circles (red circles) are the average values of beam size X (Y), and the error bars indicate the magnitude of the standard deviation. The horizontal axis of each figure is the atmospheric temperature on the optical axis.

From these results, it is clear that when the atmosphere on the optical axis of the laser beam is heated, the fluctuations in the centroid position and the beam size in the intensity distribution become large. It is considered that this is because the refractive index of the atmosphere fluctuates randomly due to the non-uniform temperature distribution. Also, the average values of centroid X and beam sizes X and Y are not so affected by heating. However, it should be noted that the average value of centroid Y shifts upward due to heating.

The temperature of the air is high near the surface of the hot plate and decreases as it rises in the height direction, so that a temperature gradient is formed. In general, heated air has a reduced density due to thermal expansion, and its refractive index is lowered [10]. Therefore, it is considered that the refractive index of air increases as the height increases from the surface of the hot plate. As a result, the optical axis of the laser beam is bent upward with a high refractive index. This is the same phenomenon as the inferior mirage that is occasionally observed on roads under the scorching sun. From these results, it can be concluded that the fluctuation of the refractive index caused by the thermal fluctuation of the atmosphere has a great influence on the propagation of light waves.

Fig. 10 shows the result of observing the interference between the signal light affected by the thermal fluctuation and the reference light that has passed through the free space. When the atmospheric temperature on the optical axis is (a) room temperature, the contrast of the signal intensity is clear and the interference is high. When the atmospheric temperature rises to (b) 30 °C, (c) 40 °C, and (d) 50 °C by heating, the signal intensity changes randomly and the interference decreases overall. The intensity distribution of signal light affected by thermal fluctuation fluctuates randomly. It is considered that the spatial mode matching efficiency with the reference light is reduced, and as a result, the interference is reduced. It is presumed that interference occurs only at the moment when the optical axes of both lights coincide.
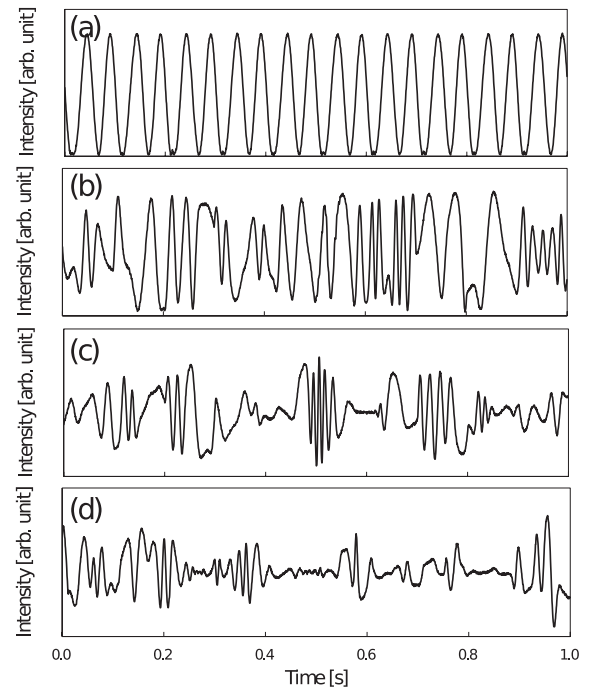
Fig. 10. Interference signal of the laser beam affected by thermal fluctuation. The temperatures on the optical axis of sigal beam are (a) room temperature 24 °C, (b) 30 °C, (c) 40°C, and (d) 50 °C, respectively.

V. EXPERIMENTAL RESULTS UNDER THE INFLUENCE OF AIR FLOW

When the laser beam passed through the atmosphere with airflow, fluctuations in the intensity distribution were observed as shown in Fig. 3(c). Compared with the case of thermal fluctuation shown in Fig. 3 (b), the change of centroid position and the distortion of beam shape are small. Similar to the thermal fluctuation experiment, the measurement results of the intensity distribution under the influence of airflow are shown in various expressions. Fig. 11 shows the centroid position of the intensity distribution in a scatter plot. Similarly, Fig. 12 is a scatter plot of the beam size of the laser beam. In each figure, (a) is the result of measurement at air volume level 0 without operating the air blower. (b), (c), and (d) represent the measurement results when the air blower is operated and the air volume level is set to 1, 2, and 3, respectively. It should be noted that the display range of centroid and beam size is expanded compared to Fig. 4 and Fig. 5.

Fig. 13 shows the frequency distribution of the centroid position of the laser beam, calculated using the measurement results of Fig. 11. Similarly, Fig. 14 is the frequency distribution of beam size, calculated using the measurement results of Fig. 12. In both figures, the air volume on the beam optical axis is (a, e) level 0 (without air flow), (b, f) level 1, (c, g) level 2, and (d, h) level 3, respectively. In Fig. 13, (a) to (d) ((e) to (h)) represent
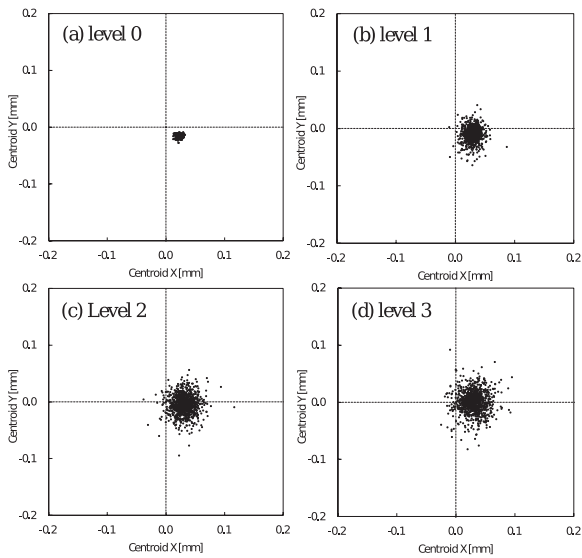
Fig. 11. Measurement result of centroid of laser beam affected by air flow. The wind speeds on the optical axis of the signal beam are (a) level 0 with air blower turned off, (b) level 1, (c) level 2, and (d) level 3, respectively.
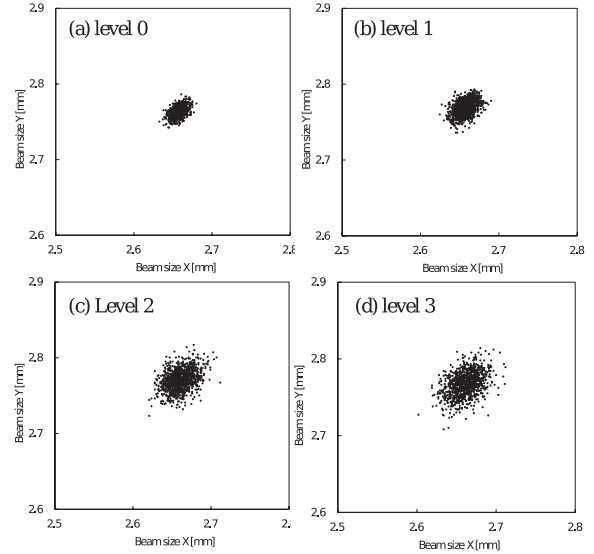
Fig. 12. Measurement result of beam size of the laser beam affected by air flow. The wind speeds on the optical axis of the signal beam are (a) level 0 with air blower turned off, (b) level 1, (c) level 2, and (d) level 3, respectively.
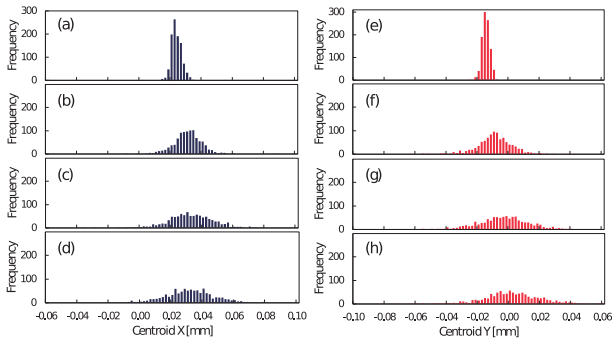
Fig. 13. Frequency distribution of centroid of laser beam affected by air flow. The air flow on the beam optical axis are (a, e) level 0 with air blower turned off, (b, f) level 1, (c, g) level 2, and (d, h) level 3, respectively. (a) to (d) show the result of centroid X, and (e) to (h) show the result of centroid Y.
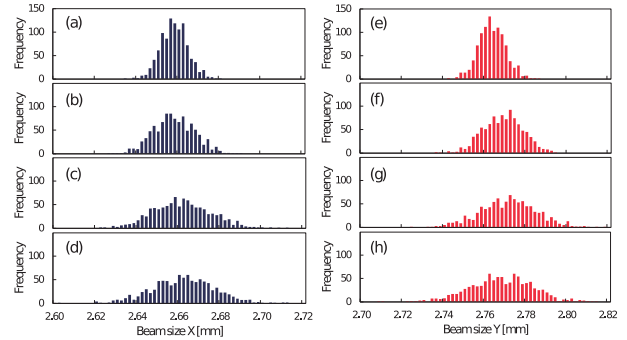
Fig. 14. Frequency distribution of beam size of laser beam affected by air flow. The air flow on the beam optical axis are (a, e) level 0 with air blower turned off, (b, f) level 1, (c, g) level 2, and (d, h) level 3, respectively. (a) to (d) show the result of centroid X, and (e) to (h) show the result of centroid Y.
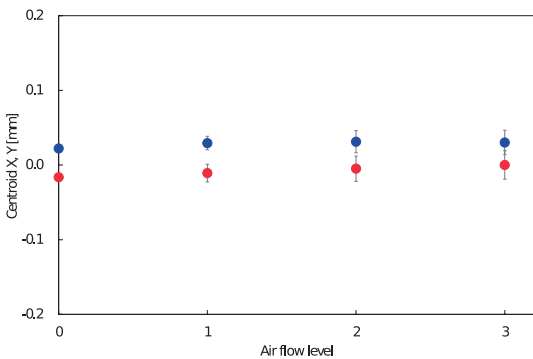
Fig. 15. Measurement result of centroid of laser beam affected by air flow. The blue circles (red circles) are the average values of centroid X (Y), and the error bars represent the standard deviation.
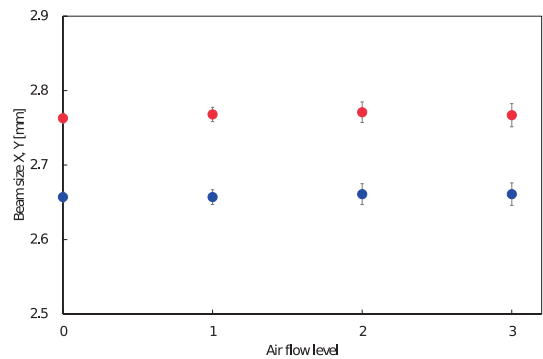
Fig. 16. Measurement result of beam size of the laser beam affected by air flow. The blue circles (red circles) are the average values of centroid X (Y), and the error bars represent the standard deviation.
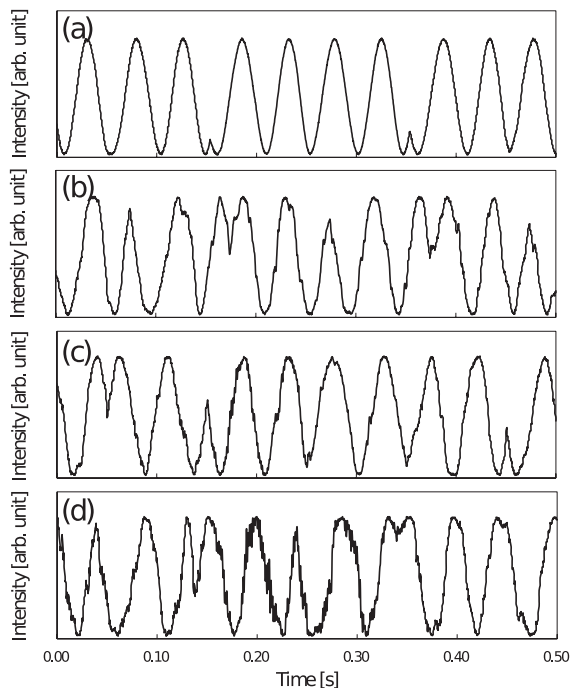
Fig. 17. Interference signal of the laser beam affected by air flow. The wind speeds on the optical axis of the signal beam are (a) level 0 with air blower turned off, (b) level 1, (c) level 2, and (d) level 3, respectively.

the frequency of centroid X (Y). Similarly, in Fig. 14, (a) to (d) ((e) to (h)) represent the frequency of beam size X (Y).

Fig. 15 and Fig. 16 are a summary of the measurement results of centroid and beam size under the influence of airflow. In Fig. 15, the blue circle (red circle) is the average value of centroid X (Y), and the error bar indicates the magnitude of the standard deviation. Similarly, in Fig. 16, the blue circles (red circles) are the average values of beam size X (Y), and the error bars indicate the magnitude of the standard deviation. The horizontal axis of each figure is the airflow level of the airflow generated by the air blower.

From these results, it can be seen that even if an air flow is generated on the optical axis of the laser beam, the centroid position of the intensity distribution and the average value of the beam size do not change much. These fluctuations increase as the air volume level of the air flow increases, but they are extremely small compared to the experimental results of thermal fluctuation. When the temperature of the air flow is the same as that of the external atmosphere, it is considered that the distribution of the refractive index on the optical axis hardly changes. Therefore, the effect of airflow on the propagation of light waves is considered to be smaller than the effect of thermal fluctuation.

Fig. 17 shows the result of observing the interference

between the signal light affected by the air flow and the reference light that has passed through the free space. When the air volume of the air flow on the optical axis is (a) level 0 (without air flow), the contrast of the signal intensity is clear and the interference is high. It can be seen that when the air volume is increased to (b) level 1, (c) level 2, and (d) level 3, the signal intensity does not change much, but the noise increases. Since the propagation characteristics of the signal light are not significantly affected by the air flow, it is considered that the spatial mode matching efficiency with the reference light does not change so much. At the same time, the fluctuation of the interference signal is increasing due to the fluctuation of the signal light. From these results, it can be concluded that the airflow does not affect the light wave interference so much, but it becomes a noise factor of the signal strength.

In this experiment, a headwind airflow was generated parallel to the optical axis. However, it is possible that the airflow in the direction perpendicular to the optical axis also affects the propagation of the light wave. In the future, we are considering experiments to verify the effects of vertical airflow.

VI. SUMMARY

For the study of quantum illumination, it is important to investigate the propagation characteristics of light waves in atmospheric disturbances. We investigated the propagation characteristics of laser light under the influence of thermal fluctuation and airflow, which are typical examples of atmospheric disturbances. It was found that the centroid position and beam size of the laser beam intensity distribution fluctuate significantly under the influence of thermal fluctuation. Such fluctuations in the intensity distribution affect the spatial mode matching efficiency between light waves, and as a result, the interference is reduced. It was confirmed that thermal fluctuation causes a non-uniform refractive index distribution and directly affects the propagation of light waves. The effect of airflow on the intensity distribution of laser light was smaller than that of thermal fluctuation. As the air volume level was increased, the noise in the interference signal increased, but the interference between the light waves did not change so much. From these results, it is considered that the distribution of the refractive index on the optical path is not so affected as long as the temperature of the airflow is the same as that of the external atmosphere. From the above results, it can be concluded that the effect of air flow on the propagation of light waves is smaller than the effect of thermal fluctuation.

VII. ACKNOWLEDGMENTS

The author is very grateful to Shyuto Mizutani, Yuto Murayama, and Kazuki Sekimen, students of the Department of Information and Communication Technology,

REFERENCES

[1] S. Lloyd, "Enhanced sensitivity of photodetection via quantum illumination," Science **321** 1463-1465, (2008).

[2] S. H. Tan, B. I. Erkmen, V.Giovannetti, S. Guha, S. Lloyd, L. Maccone, S. Pirandola, and J. H. Shapiro,"Quantum illumination with Gaussian states," Phys. Rev. Lett. **101** 253601, (2008).

[3] J. H. Shapiro, and S. Lloyd, "Quantum illumination versus coherent-state target detection," New J. of Phys. **11** 063045, (2009).

[4] G. Masada, "Verification of quantum entanglement of two-mode squeezed light source towards quantum radar and imaging ," Proc. SPIE **10409** Quantum Communications and Quantum Imaging XV, 104090P, (2017).

[5] G. Masada, "A study of laser beam propagation through 10 meters length of a fog," Tamagawa University Quantum ICT Research Institute Bulletin, Vol.**9**, No.1, 41-43, (2019)

[6] G. Masada, "Investigation of light wave propagation in atmospheric disturbance toward quantum illumination," Proc. SPIE **11835** Quantum Communications and Quantum Imaging XIX, 118350E, (2021).

[7] L. A. Chernov, "Wave Propagation in a Random Medium," McGraw-Hill, New York, 1960.

[8] V. I. Tatarski, "Wave Propagation in a Turbulent Medium," Dover Publications Inc., 1968.

[9] L. C. Andrews, and R. L. Phillips, "Laser Beam Propagation through Random Media," 2nd ed., SPIE Press, 2005.

[10] J. C. Owens, "Optical refractive index of air: Dependence on pressure, temperature and composition," Appl. Optics **6** 51-59, (1967).